# Interaction of Se and GaSe with Si(111)

Shuang Meng, B. R. Schroeder, and Marjorie A. Olmstead
*Department of Physics, University of Washington, Box 351560, Seattle, Washington 98195*
(Received 5 August 1999; revised manuscript received 7 December 1999)

Deposition of Se and GaSe on Si(111)7×7 surfaces was studied with low-energy electron diffraction, x-ray photoelectron spectroscopy, and x-ray photoelectron diffraction to probe initial nucleation and interface structure for GaSe/Si(111) heteroepitaxy. Room-temperature deposition of Se on Si(111)7×7 results in an amorphous film. Subsequent annealing leads to Se evaporation without ordering or interdiffusion. Se deposition at 450°C saturates at submonolayer coverage with no diffusion of Se into the substrate. There is no clear evidence of ordered sites for the Se. Growth of GaSe on Si(111)7×7 above 500°C results in a pseudomorphic bilayer, with Si-Ga-Se bonding. Additional GaSe does not stick to the bilayer above 525°C. The resulting Se lone pair at the surface leads to an ideally passivated surface similar to As/Si(111). This stable surface is similar to the layer termination in bulk GaSe. The single domain bilayer is oriented with the Ga-Se bond parallel to the substrate Si-Si bond.

Interface formation during the initial stage of heteroepitaxial growth plays a crucial role in controlling the subsequent growth of the overlayer. The interface formation mechanism and resultant structure are determined not only by physical parameters of the grown material and the substrate, such as lattice symmetry and mismatch, but also by chemical reactions taking place between overlayer constituents and the substrate. Two key issues common to most compound heteroepitaxial growth systems are interface bonding and interdiffusion: When *AB* is deposited on *C*, do *AC* or *BC* bonds form, and do *A* or *B* atoms diffuse into the substrate? In this paper, we address these questions with an x-ray photoelectron diffraction study of the interaction of Se and GaSe with Si(111)7×7.

Semiconductors based on III-VI compounds have been receiving increasing attention recently due to their many unique structural, electronic, and optical properties not found in group IV and III-V materials.[1–3] Ga-Se compounds exhibit two stable bulk stoichiometries: layered GaSe and cubic $Ga_2Se_3$. Both exhibit a basic structural building block of a hexagonal Ga-Se bilayer, although 1/3 of the Ga sites are empty in the cubic form. The hexagonal GaSe lattice spacing is 2.4% smaller than that of Si(111), whereas $Ga_2Se_3$ is lattice matched to Si within 0.3%. Several groups have reported growth of layered GaSe on Si(111).[4–10] Most of these studies concentrated on film morphology and crystallinity. One group has studied interface structure with x-ray standing wave fluorescence,[8,9] and deduced Si-Ga bonding and mixed orientation of the first bilayer. A single interface environment for Ga and Se was also inferred from soft x-ray photoelectron spectroscopy on sequentially annealed epitaxial films.[11]

The role of Se interface reactions in GaSe/Si(111) is unknown. Selenium plays a key role in the initial nucleation of GaSe/GaAs(111) (Ref. 12) and ZnSe/Si(100).[13] In both cases, Se both terminates the surface and diffuses into the substrate. In the case of ZnSe/Si(100), the resultant amorphous $SiSe_x$ prevents nucleation of crystalline ZnSe. These reactions are observed for both Se and compound deposition. In contrast to these systems, however, we find that Se does not play the same key role in the initial nucleation of GaSe on Si(111). Below about 425°C, we form an amorphous film, with no Se interdiffusion, for both GaSe and Se deposition. At higher temperatures, less than one monolayer of Se sticks. GaSe growth above 500°C starts with a GaSe bilayer in which the interface bonding is between Ga and Si. This bilayer passivates the substrate dangling bonds and forms an ideally terminated surface similar to Si(111):As.[14,15] It provides an ordered substrate for further film growth, although we find that additional GaSe does not stick above 525°C.

Commercial *n*-type Si(111) wafers ($\rho \sim 1\Omega$ cm) were chemically treated to form a thin oxide layer. The samples were outgassed in ultrahigh vacuum (UHV) at 500°C for at least 3 h, and then flashed to 875°C several times until a well-ordered 7×7 low-energy electron diffraction (LEED) pattern was observed. The samples were resistively heated by direct current. Sample temperatures were monitored with an optical pyrometer. X-ray photoelectron spectroscopy (XPS) showed no surface oxygen or carbon.

Se depositions were performed using a Se electrochemical cell, while GaSe depositions were performed using a GaSe Knudsen cell (deposition chamber base pressure $7\times10^{-11}$ torr). Samples were annealed at the growth temperature for 30 s after blocking the source. Samples were transferred under UHV to the analysis chamber (base pressure $1\times10^{-10}$ torr) for LEED and x-ray photoemission spectroscopy and diffraction (XPS/XPD). XPS/XPD was performed using Mg $K_\alpha$ x rays (1253.6 eV) and a Leybold EA-11 hemispherical analyzer. The angle between the incident photons and detected electrons is fixed at 55° in the horizontal plane. The sample rotates around the vertical axis ($\theta$) and the sample normal ($\phi$).

XPD has been developed to probe local atomic structures near surfaces.[16,17] For high kinetic energy electrons, forward focusing dominates the process of internuclear scattering, while low-energy photoelectrons also exhibit strong back- and multiple-scattering. The resultant diffraction pattern may be used to obtain structures of heteroepitaxial films and to measure interdiffusion. XPD's elemental specificity enables separate structural determination of each individual element's environment.

 

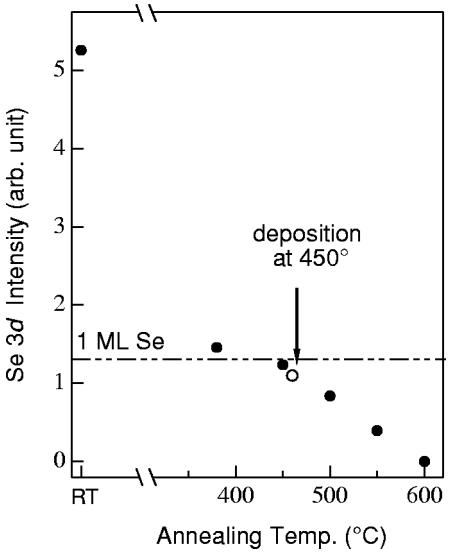


FIG. 1. Measured Se $3d$ intensities (arbitrary units, normal emission) for Se grown on Si(111) at room temperature and subsequently annealed at successive higher temperatures (closed circle). The open circle corresponds to direct deposition of Se on Si(111) at 450°C. The dashed line indicates the Se $3d$ intensity of GaSe bilayer (see Fig. 4).

*Se/Si*(111). Understanding interface formation for GaSe/Si(111) growth requires knowledge about reactions of each individual element with Si(111). The interaction of elemental Ga with Si(111) is well known: at 1/3 monolayer coverage, it forms a $\sqrt{3}\times\sqrt{3}$ surface reconstruction;[18] at higher coverages, a discommensurate $6.3\times6.3$ layer is formed.[19] In contrast, the interaction of Se with Si(111) is not well understood, with no reports under molecular-beam-epitaxy conditions (elevated temperature and ultrahigh vacuum). Dev *et al.*[20] studied Se adsorption from a weakly acidic methanol solution on chemically cleaned Si(111) and (220) surfaces at room temperature (RT). Based on their x-ray standing wave fluorescence results, they proposed Se atoms occupy bridge sites on a Si(111) surface, although the fraction of Se atoms in those sites was small. Bringans and Olmstead investigated the interaction of Se with clean Si(100) in UHV.[13,21] Their photoemission results showed that annealing room-temperature deposited Se to 300°C results in formation of $SiSe_2$, suggesting Se-Si interdiffusion, while higher temperature annealing results in submonolayer Se in bridge sites. In this section, we report on direct deposition of Se on clean Si(111)$7\times7$ both at room temperature and at temperatures typical of GaSe heteroepitaxy. In contrast to Si(100),[13,21] we find no clear evidence of either an ordered site or interdiffusion.

Figure 1 shows the Se $3d$ core-level intensity for Se deposited on Si(111)$7\times7$ at room temperature (RT) and subsequently annealed to successively higher temperatures. Above ~400°C, only submonolayer Se remains on the surface. It is fully removed by ~600°C, although the $7\times7$ low-energy electron diffraction (LEED) pattern is not yet visible at this temperature. Also shown in Fig. 1 are the Se $3d$ intensities for Se deposited at 450°C and for a GaSe bilayer (one ML Se) deposited at 525°C (see below). Both are independent of total exposure to Se flux (beyond 1 ML), indicating saturation coverage has been reached. Both Se

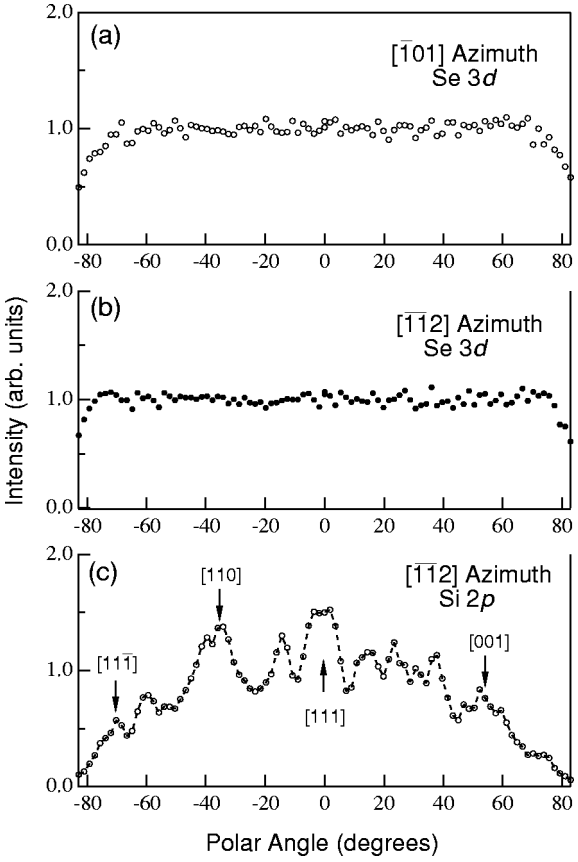


FIG. 2. XPD scans of Mg $K_\alpha$-excited Se $3d$ core-level photoemission (KE=1195 eV) along (a) $[\bar{1}01]$ and (b) $[\bar{1}\bar{1}2]$ azimuths for Se deposited at 450°C on Si(111)$7\times7$. For reference, the substrate Si $2p$ (KE=1150 eV) XPD scan along the $[\bar{1}\bar{1}2]$ azimuth is shown in (c).

preparations — RT+450°C anneal and direct 450°C deposition — exhibit diffuse $1\times1$ LEED patterns. They frequently exhibit faint 1/7 rosettes around each $1\times1$ spot, suggesting remnant substrate $7\times7$ reconstruction. LEED indicates that Se adsorption does not lead to a well-ordered surface, at least for deposition at 450°C.

To investigate possible Se interdiffusion and/or local ordering, we performed XPD on the Se/Si(111) samples. Figure 2 shows Se $3d$ XPD along two high symmetry azimuths, $[\bar{1}\bar{1}2]$ and $[\bar{1}01]$, for 450°C Se deposition. The substrate Si $2p$ XPD along $[\bar{1}\bar{1}2]$ is also shown in the figure for comparison. XPD at this high kinetic energy (1195 eV) is dominated by forward focusing. The absence of observed diffraction peaks indicates Se atoms either reside in the top layer or are buried in disordered sites. The absence of $\cos\theta$ attenuation at high polar angles (the cutoff beyond ~75° is due to sample holder shadowing) suggests that all Se atoms remain in the top layer and no interdiffusion has occurred. This conclusion is confirmed by the polar profile at lower kinetic energy (Se $2p$ 48 eV),[24] where the inelastic scattering length (escape depth ~6 Å) is much shorter.

Overall, both high- and low-energy XPD, as well as LEED, are consistent with a disordered surface Se layer with little or no interdiffusion. The structure is independent of whether the Se is deposited at room temperature and annealed, or deposited directly at elevated temperature.

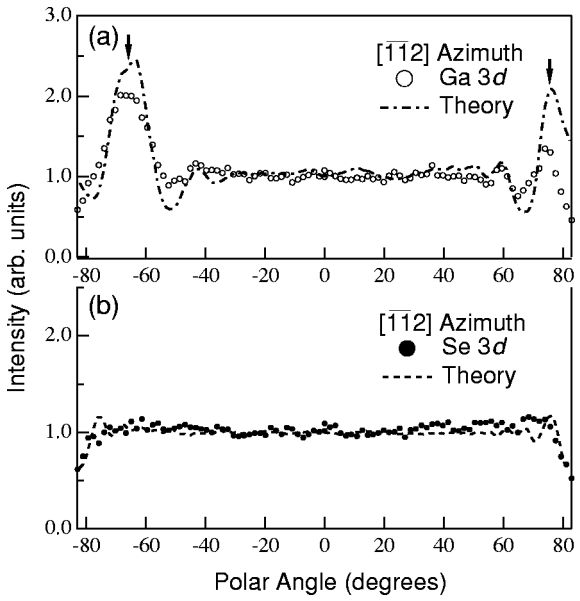


FIG. 3. (a) Polar scan of Ga $3d$ (KE=1230 eV) intensity along the $[\overline{1}12]$ azimuth after deposition of GaSe on Si(111)$7\times7$ at 550°C. The arrows indicate the two diffraction peaks. The dashed curve corresponds to the calculated diffraction pattern based on the structural model shown in Fig. 4. (b) Polar scan of Se $3d$ (KE =1195 eV) intensity along $[\overline{1}12]$ and the corresponding calculated diffraction pattern.

*GaSe/Si*(111). Ga-Se was grown on Si(111)$7\times7$ at various substrate temperatures using a stoichiometric GaSe source, which evaporates as $Ga_2Se+1/2Se_2$.[22] The film was then analyzed by LEED and XPS/XPD. Growth of Ga-Se on Si(111) falls into three distinct regimes as the substrate temperature $T_s$ varies. Polycrystalline film growth was achieved for 425°C$<T_s<$500°C. Below 425°C, LEED shows the resulting film to be amorphous. Growth at $T_s>$500°C leads to formation of a GaSe bilayer; additional GaSe does not stick above 525°C. In this section we focus on the GaSe bilayer structure, which both passivates the surface and serves as a template for ordered GaSe growth.

Figure 3 shows Ga $3d$ and Se $3d$ XPD for a GaSe (bilayer) film grown at 550°C. The Se $3d$ emission shows flat modulation with no strong diffraction peaks, similar to Fig. 2. Low-energy electron diffraction after growth shows strong, sharp $1\times1$ spots, in contrast with the faint, diffuse $1\times1$ structure obtained after Se adsorption. The combination of LEED and XPD indicates that Se atoms are sitting in ordered sites in the top layer, with no scatterers above them. In contrast, the Ga $3d$ emission shows two strong diffraction peaks: 64° from normal emission toward $[11\overline{2}]$, and 77° from normal toward $[\overline{1}12]$. No diffraction peaks are observed at normal emission, indicating no bulk GaSe has nucleated.

A structural model consistent with the XPD results is shown in Fig. 4, in which Ga bonds to the surface Si and each Se bonds with three Ga atoms underneath it. The two Ga $3d$ diffraction peaks correspond to scattering along the Ga-Se bond ($-64°$) and scattering from the Se opposite to the bond (77°). Also shown in Fig. 3 are predicted XPD patterns for the structure shown in Fig. 4, using multiple-scattering cluster calculations (MSCD code[23]). Notice that the

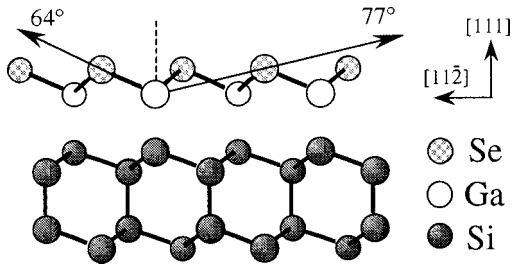


FIG. 4. Schematic of the GaSe bilayer structure on the Si(111) substrate deduced from the XPD polar scans shown in Fig. 3. The arrows indicate the directions corresponding to the two strong forward-focusing peaks for Ga $3d$.

peak at 77° is attenuated in the experimental polar scan due to the shadowing effect of sample holder beyond 75°. Electron counting based on this structural model shows each Ga donates one valence electron to the Ga-Si interface bond and two electrons to three Ga-Se bonds, while the Se donates four electrons to the Ga-Se bonds leaving a lone pair at the surface. This structure terminates the substrate dangling bonds and results in a fully passivated surface, similar to As terminated Si(111).[14,15] Like Si(111):As, we find Si(111):GaSe is highly resistant to contamination, collecting no oxygen or carbon after extended periods (days) in the UHV chamber. The structure is also identical to one-half a layer in bulk GaSe. The observed Ga-Se angle (64°) is closer to that of bulk GaSe (63°) than Si-As (66°) in Si(111):As (Ref. 15) or bulk Si-Si (70°).

The bilayer structure has a single domain, indicated by the asymmetry in the Ga $3d$ diffraction pattern. Comparison with the Si $2p$ XPD of the substrate shows Ga-Se bonds oriented approximately parallel to substrate Si-Si bonds, as indicated in Fig. 4. However, the exact position of the Ga atom relative to substrate surface Si cannot be deduced from the measured Ga $3d$ and Se $3d$ XPD patterns. Koëbel *et al.* used x-ray standing-wave fluorescence (XSWF) to study the epitaxial growth of GaSe ultrathin films on Si(111) at 450°C.[9] They proposed a similar interface model, and determined the Ga to be located directly above Si. However, they inferred two domains: one with ''Si-like'' structure (Fig. 4), and the other with ''GaSe-like'' structure corresponding to a 180° rotation.[9] In contrast, our XPD study shows a single domain bilayer, at least for deposition above 500°C. These differences may be associated with different growth conditions. The XSWF study used elemental sources with Se/Ga flux ratio between 8 and 9, in contrast to our stoichiometric source. At 450°C, we observed a polycrystalline film, consistent with the two orientations observed with XSWF.

Low kinetic energy XPD patterns have also been obtained for both structures reported in this paper; the results, including theoretical modeling, will be published elsewhere.[24] For both Si(111)-Se and Si(111)-GaSe, the results are consistent with all conclusions drawn above. In particular, no strong diffraction features are observed for Si(111)-Se, and all structural measurements on the GaSe bilayer support the model in Fig. 4.

In summary, we found Se adsorption on Si(111) at 450°, either directly or as RT deposition followed by annealing,

leads to a disordered Se submonolayer on the surface with no interdiffusion. Growth of GaSe on Si(111) above 500°C forms a single-domained GaSe bilayer with a very low sticking coefficient on the bilayer above 525°C. The bilayer-substrate bond is between Ga and Si, with Se bonded to interface Ga. This bilayer effectively passivates the substrate dangling bonds and leaves Se lone pair states on the surface. The bilayer plays a crucial role in controlling initial nucleation of GaSe.

We thank F. S. Ohuchi, Z. R. Dai, and A. Bostwick for useful discussions. This work was supported by NSF Grant No. DMR9801302 and DOE Grant No. DE-FG03-97ER45646/A003.

[1] N.C. Fernelius, Prog. Cryst. Growth Charact. Mater. **28**, 275 (1994).
[2] F. S. Ohuchi and M. A. Olmstead, in *Wiley Encyclopedia of Electrical and Electronics Engineering*, edited by J. G. Webster (Wiley, New York, 1999), Vol. 19, p. 147.
[3] A. Koma, K. Sunouchi, and T. Miyajima, J. Vac. Sci. Technol. B **3**, 724 (1985).
[4] K.Y. Liu, K. Ueno, Y. Fujikawa, K. Saiki, and A. Koma, Jpn. J. Appl. Phys., Part 2 **32**, L434 (1993).
[5] L.T. Vinh, M. Eddrief, C. Sébenne, A. Sacuto, and M. Balkanski, J. Cryst. Growth **135**, 1 (1994).
[6] J.E. Palmer, T. Saitoh, T. Yodo, and M. Tamura, J. Cryst. Growth **147**, 283 (1995).
[7] A. Koëbel, Y. Zheng, J.F. Pétroff, M. Eddrief, L.T. Vinh, and C. Sébenne, J. Cryst. Growth **154**, 269 (1995).
[8] Y. Zheng, A. Koëbel, J.F. Pétroff, J.C. Boulliard, B. Capelle, and M. Eddrief, J. Cryst. Growth **162**, 135 (1996).
[9] A. Koëbel, Y. Zheng, J.F. Pétroff, J.C. Boulliard, B. Capelle, and M. Eddrief, Phys. Rev. B **56**, 12 296 (1997).
[10] N. Jedrecy, R. Pinchaux, and M. Eddrief, Phys. Rev. B **56**, 9583 (1997).
[11] A. Amokrane, C.A. Sébenne, A. Cricenti, C. Ottaviani, F. Proix, and M. Eddrief, Appl. Surf. Sci. **123/124**, 619 (1998).
[12] L.E. Rumaner, M.A. Olmstead, and F.S. Ohuchi, J. Vac. Sci. Technol. B **16**, 977 (1998).
[13] R.D. Bringans and M.A. Olmstead, Phys. Rev. B **39**, 12 985 (1989).
[14] M.A. Olmstead, R.D. Bringans, R.I.G. Uhrberg, and R.Z. Bachrach, Phys. Rev. B **34**, 6041 (1986).
[15] R.I.G. Uhrberg, R.D. Bringans, M.A. Olmstead, R.Z. Bachrach, and J.E. Northrup, Phys. Rev. B **35**, 3945 (1987).
[16] C.S. Fadley, Surf. Sci. Rep. **19**, 231 (1993).
[17] S.A. Chambers, Surf. Sci. Rep. **16**, 261 (1992).
[18] J. Zegenhagen, J.R. Patel, P. Freeland, D.M. Chen, J.A. Golovchenko, P. Bedrossian, and J.E. Northrup, Phys. Rev. B **39**, 1298 (1989).
[19] J. Zegenhagen, M.S. Hybertsen, P.E. Freeland, and J.R. Patel, Phys. Rev. B **38**, 7885 (1988).
[20] B.N. Dev, T. Thundat, and W.M. Gibson, J. Vac. Sci. Technol. A **3**, 946 (1985).
[21] R.D. Bringans and M.A. Olmstead, J. Vac. Sci. Technol. B **7**, 1232 (1989).
[22] A. Ludviksson, L.E. Rumaner, J.W. Rogers, Jr., and F.S. Ohuchi, J. Cryst. Growth **151**, 114 (1995).
[23] Y. Chen, F.J. García de Abajo, A. Chassé, R.X. Ynzunza, A.P. Kaduwela, M.A. Van Hove, and C.S. Fadley, Phys. Rev. B **58**, 13 121 (1998).
[24] S. Meng, B. R. Schroeder, A. Bostwick, E. Rotenberg, and M. A. Olmstead (unpublished).